

Supplementary materials

(Prestipino A et al. Oncogenic JAK2^{V617F} causes PD-L1 expression mediating immune-escape in myeloproliferative neoplasms)

Supplementary Materials and Methods:

Mice

Rag2^{-/-}Il2r^{-/-} mice were bred in the animal facility at Freiburg University Medical Center (Freiburg, Germany). BALB/c (H-2K^d), C57BL/6 (H-2K^b), and C3H (H-2K^k) mice were purchased from the animal facility at Freiburg University Medical Center or from Janvier Labs. *Pd-1^{-/-}* mice on a C57BL/6 background were kindly provided by Prof. R. Schrimbeck (Universitätsklinikum Ulm, Germany). The conditional floxed JAK2 (*JAK2FLEX/+ or L2/+*) knock-in mice on C57BL/6 background were a kind gift from Dr. Villeval (Inserm, U.1009, Villejuif, France). These floxed JAK2 L2-mice were crossed with Cre deleter mice (C57BL/6 NCRL Rosa26 Cre Del, The Jackson Laboratory) to generate mice with a constitutively active JAK2^{V617F} mutation. The *Jak2^{V617F} x E2ACre* knock-in mouse model was provided by S.L. (13). All mice were housed under specific pathogen-free (SPF) conditions at the ZKF mouse facility of the University Medical Center Freiburg and used between 6-12 weeks of age. All animal protocols (G-13/116, G-16/018; X-13/07J; X-15/10A) were approved by the Federal Ministry for Nature, Environment and Consumer Protection of the state of Baden-Württemberg, Germany and protocol A11605M and p1382 by QIMR Berghofer.

Transplantation models and antibody treatment

PBMCs were isolated by Ficoll gradient centrifugation, according to the manufacturer's protocol (Sigma-Aldrich). For the xenotransplantation model, $10\text{-}40 \times 10^6$ human PBMCs isolated from MPN patients were intravenously injected into *Rag2^{-/-}Il2r^{-/-}* mice. The transplanted PBMCs contained donor T cells as effector cells (98% donor genotype) and CD45⁺ cells (50% recipient genotype) as potential MPN target cells. Mice were treated on day 8 with 250 μg of either anti-human PD-1 antibody (clone J116, BioXCell) or mouse IgG1 isotype control (clone MOPC-21, BioXCell). For the depletion of CD3⁺ cells, total PBMCs were incubated with anti-human CD3 beads (CD3 MicroBeads human, MACS Miltenyi Biotec), after which the CD3-depleted cells were isolated by magnetic sorting, according to the manufacturer's protocol. For the bone marrow transplantation model, BALB/c donor mice were treated with 5-FU and then sacrificed on day 4 after treatment. Bone marrow cells were isolated and infected with an empty vector, JAK2^{V617F} GFP⁺ vector, or JAK2^{FERM-deleted} GFP⁺ vector. Recipient mice underwent TBI (6.5 Gy) and were then transplanted with 0.4×10^6 bone marrow cells (40% GFP⁺). Mice were treated i.p. with an anti PD-1 antibody (clone J43, mAb provided by B.R.B.) or Armenian hamster isotype control (BioXCell) on days 19, 27, 34, 42 after transplantation. For the analysis of the T cell compartment, some mice were treated i.p. with 250 μg anti PD-L1 antibody (clone 10F.9G2, BioXCell) or Rat IgG2b isotype control (clone LTF-2, BioXCell) on days 4, 8, 12, 16 after transplantation, and then sacrificed on day 19. Antibodies are listed in table S3.

qPCR for JAK2^{V617F} allele burden

Genomic DNA isolated from PBMCs was used for qPCR. The JAK2^{V617F} allele burden was calculated as follows: $\text{JAK2}^{\text{V617F}} \text{ in } \% = \text{JAK2}^{\text{V617F}} \text{ copy numbers} / (\text{JAK2}^{\text{V617F}} \text{ copy numbers} + \text{JAK2-WT copy numbers}) * 100$. Gene copy numbers were measured by qPCR.

Cell lines and in vitro treatments

The following murine cell lines were used: Ba/F3 cells (provided by S.G., and 32D cells (provided by F.H.). The 32D cells (15) were previously transfected with the receptor for human erythropoietin (EPO) and JAK2 WT (Epo-dependent cells) or JAK2^{V617F} (EPO-independent cells). Before the experiments, 32D cells with JAK2 WT underwent EPO starvation for 30-40 hours, to shut down JAK2 signaling. The viability of the starved cells was assessed after each starvation and shown to be comparable with the viability of the JAK2^{V617F} Epo-independent cell line. The human cell lines UKE-1, SET-2, and MUTZ-8 were bought from ATCC, and K562 was provided by C.M.. The K562 cells we used express the ecotropic retrovirus receptor (21).

All cell lines were tested repeatedly for Mycoplasma contamination and were found to be negative.

The cells were cultured in RPMI 1640 (Sigma-Aldrich) supplemented with 10% FCS, 100 U/mL penicillin, and 0.1 mg/ml streptomycin. The medium for Ba/F3 cells transfected with the empty vector and with JAK2-WT was supplemented with recombinant murine IL-3 (PeproTech) at a final concentration of 20 ng/ml. The medium for 32D cells was supplemented with recombinant human EPO (Epoetin alfa HEXAL) at the final concentration of 1 U/mL. The human cell lines were cultured in the same medium described for the Ba/F3 cells (SET-2, K562, MUTZ-8), or in IMDM (Sigma-Aldrich) supplemented with 10% FCS, 10% horse serum, 10^{-6} M hydrocortisone (Sigma-Aldrich), 100 U/mL penicillin, and 0.1 mg/ml streptomycin (UKE-1). Cells were exposed to ruxolitinib (Novartis Pharma) for 24 hours, the specific JAK2 inhibitor SD-1029 (Merck Millipore) for 48 hours, the specific STAT3 inhibitors S3I-201 or C188-9 (Merck Millipore) for 48 or 16 hours,

respectively, or the specific STAT5 inhibitor pimozide (Merck Millipore) for 6 hours. Where indicated, Ba/F3, 32D, or K562 cells were additionally infected with retroviral constructs containing STAT1/3/5 GOF or LOF mutations. Briefly, Plat-E packaging cells [cultured in Dulbecco's Modified Eagle Medium (DMEM), Life Technologies] were transfected using TurboFect Transfection Reagent (Thermo Scientific), according to the manufacturer's protocol. The cells were incubated with RPMI 1640 supplemented with 10% FCS, 100 U/mL penicillin, and 0.1 mg/ml streptomycin 24 hours after transfection, and then the medium (containing virus) was harvested 3 times, every 12 hours. Recipient cells were seeded at 0.3×10^6 cells/ml, infected 3 times every 12 hours by adding the virus-containing medium and polybrene (Sigma-Aldrich) to a final concentration of 4 $\mu\text{g/mL}$ (for 32D and K562 cells) or 8 $\mu\text{g/mL}$ (for Ba/F3 cells), and centrifuged 15 minutes at 1500 rpm at room temperature.

Luciferase promoter assay

The SV40 promoter was removed from the Luciferase Reporter Vector pGL4.13 [luc2/SV40] (Promega) by restriction digest using BglII and HindIII. Subsequent blunt-end ligation of the promoterless pGL4.13 was performed. The sequence of the PD-L1 promoter was PCR-amplified from genomic DNA of the human HEL erythroleukemia cell line and cloned into the pGL4.13[luc2/SV40] vector using SacI and XhoI after removal of the SV40 promoter. The oligonucleotide sequences used for PCR amplification of the PD-L1 promoter are provided in table S4. DNA purifications were performed using GeneJET PCR Purification Kit (Thermo Scientific). For plasmid extractions, we used NucleoSpin Plasmid EasyPure and NucleoBond Xtra Midi/Maxi kits (MACHEREY-NAGEL). The vector systems used for measurement of PD-L1 promoter activity are displayed in fig. S5. The luciferase assay was performed as follows: After cultivation for 24 hours, 2×10^6 cells from human MPN cell lines (K562 and HEL) were co-transfected with 2 μg of the pGL4.13 luciferase construct (empty

vector or pGL4.13-PD-L1 promoter) and the Renilla Luciferase Control Reporter Vector (Promega) at a ratio of 1:10 (200 ng) using the Amaxa Cell Line Nucleofector Kit V (Lonza). 5×10^5 of the transfected cells were seeded in 1 ml growth medium in a 24-well plate. After 24 hours, luminescence of firefly and Renilla luciferase in untreated cells was quantified by the Dual-Luciferase Reporter Assay System (Promega) on the TriStar LB 941 Multimode Microplate Reader (Berthold Technologies). Values were normalized by dividing them by Renilla luciferase activity.

Treatment with the specific JAK2 inhibitor SD-1029, the STAT3 inhibitor S3I-201, or the equivalent volume of DMSO was performed 2 hours after electroporation. The treated cells were then incubated for an additional 24 hours, and luminescence was measured as described above.

DNA constructs

To generate the *STAT1* mutations, *STAT1* was amplified and isolated from Jurkat cell cDNA by PCR. Point mutations within the *STAT1* gene were generated by PCR-based site-directed mutagenesis and addition of restriction sites for BamHI and KpnI. PCR fragments were cloned into the pJET cloning vector (Thermo) and Sanger sequenced (Seqlab). The *STAT1* gene was cut with BamHI and KpnI (New England Biolabs) and cloned into pcDNA3.1(+) vector. The primer sequences used are provided in table S5. For subcloning in the pMx-Ires-GFP vector, the pMx-Ires-GFP vector was digested with BamHI. pcDNA3.1(+)-*STAT1* was digested with KpnI. Both restriction sites were blunted before being digested again with NcoI. Ligation was done according to the manufacturer's instructions (New England Biolabs). Correct insertions were determined by control digestion and sequencing.

STAT3 mutations used for generating the STAT3 LOF and GOF vectors were published previously (16).

The *STAT5* mutations used for generating the STAT5 GOF vectors were published previously (17). pMX-Ires-GFP and pMX-STAT5b were cut with NotI and EcoRI. The *STAT5b* insert was analyzed for its size and purified by gel extraction followed by ligation in the pMX-IRES-GFP according to the manufacturer's instructions (New England Biolabs).

Western blotting

Murine Ba/F3 and 32D cells (transfected as previously described (14)) were left untreated or treated with the specific JAK2 inhibitor SD-1029 for 24 or 48 hours as mentioned in the figure legends and lysed using a radioimmunoprecipitation assay buffer (Santa Cruz Biotechnology) supplemented with Phosphatase Inhibitor Cocktail 2 (Sigma-Aldrich). Protein concentrations were determined using the Pierce BCA Protein Assay Kit (Life Technologies). After running and resolving the total proteins in 4% to 12% sodium dodecyl sulfate-polyacrylamide electrophoresis gels (NuPAGE, Invitrogen), the protein samples were transferred onto PolyScreen PVDF Hybridization Transfer Membranes (PerkinElmer). After blocking with blocking buffer (5% BSA in 1X Tris-buffered saline containing 0.1% Tween-20), the primary antibodies diluted in blocking buffer were added to the membrane. The primary antibodies used were against phospho-JAK2 (Tyr1007/1008, #3771), JAK2 (D2E12, #3230), STAT3 (79D7, #4904), phospho-STAT3 (Tyr705, #9131), STAT1 (#9172), phospho-STAT1 (Tyr701, #9167), STAT5 (D206Y, #94205), and phospho-STAT5 (Tyr694, #9359). β -actin (13E5, #4970) was used as a loading control. All antibodies were purchased from Cell Signaling Technology. As a secondary antibody, we used horseradish peroxidase (HRP)-linked anti-rabbit IgG (#7074, Cell Signaling Technology). Lumigen ECL Plus (Lumigen) was used as the chemiluminescent substrate, and the blot signals were detected using the ChemoCam Imager 3.2 (Intas Science Imaging Instruments GmbH) and quantified using LabImage 1D software.

Flow cytometry

The fluorochrome-conjugated antibodies that were used for flow cytometric analysis are shown in detail in table S3. The intracellular staining was done using BD Cytofix/Cytoperm kit (BD Biosciences). For analysis of pSTAT3, cells were fixed with 2% formalin and then exposed to 90% methanol before application of the pSTAT3 antibody. Propidium iodide staining was done for cell cycle analysis. Before analysis, cells were stained for CD3 and fixed in ethanol. After being washed in PBS, they were incubated in 5 µg/ml propidium iodide (Molecular Probes) containing 100 µg/ml RNase A (Sigma) for 30 minutes at 37°C. Cell cycle distribution analysis was done using FlowJo Software (FlowJo LLC) and the Watson (pragmatic) algorithm. To examine cell viability and exclude dead cells, we used the LIVE/DEAD Fixable Dead Cell Stain kit (Molecular Probes). Data were acquired on a CyAn ADP and BD LSR Fortessa flow cytometer (Beckman Coulter) and analyzed using FlowJo software. In JAK2^{V617F} murine CD41 cells, the difference between PD-L1 and isotype antibody was calculated and expressed as fold change relative to WT control. The fold change in MFI for PD-L1 surface expression was calculated by setting the median value of fluorescence intensity for PD-L1 derived from all healthy individuals as 1 and then listing the values from the MPN patients relative to that.

Immunohistochemical analysis of bone marrow biopsies

Formalin-fixed and paraffin-embedded bone marrow biopsies were decalcified in an EDTA solution. After heat-induced antigen retrieval of the 2 µm sections (cooking in retrieval buffer “high” by DAKO for 6 minutes), PD-L1 staining was performed using a rabbit anti-human PD-L1 antibody (monoclonal, SP263, Ventana Medical Systems, ready to use, 30 minutes

incubation time) and the EnVision Flex-Kit (DAKO) for signal visualization. The staining results were quantified by assessing the number of PD-L1 positive cells as a proportion of a total of 300 nucleated bone marrow cells, which were obtained by examining 100 cells each in three different high power fields (400x original magnification) of the respective tissue slide. As a control, bone marrow biopsies were stained with an alternative PD-L1 antibody (monoclonal rabbit anti human PD-L1, E1K3N, Cell Signaling, 1:50, 30 minutes incubation time) showing the same staining pattern with a slightly lower signal intensity. For pSTAT3 staining of human bone marrow, we used anti-p-STAT3 antibody (γ 705; D3A7 XP, rabbit mAB /Lot. 31, Cell Signaling #9145).

TCR sequencing

To study the clonal expansion of T cells, mice with JAK2^{V617F} transfected bone marrow were treated with 250 μ g of anti-PD-L1 antibody (or corresponding isotype control) on days 3, 6, and 9 after transplantation, and sacrificed on day 12. RNA from sorted CD4⁺ and CD8⁺ T cells was isolated using the RNeasy Mini kit (QIAGEN). Sequencing of the TCR α and β chains was performed on RNA by using a modified rapid amplification of cDNA-ends with polymerase chain reaction (RACE) PCR protocol. cDNA was synthesized using the SmartScribe enzyme (Clontech) in the presence of biotinylated primers specific for the constant α and β chain genes and of a barcoded (5 bp) template switching primer. TCR-specific cDNA molecules were captured with streptavidin magnetic beads (Dynabeads, Life Technologies), washed, and resuspended in 10 μ l water. 1 μ l cDNA and 1 μ l first PCR product were used as input material for the first and second exponential PCR, respectively. Fusion primers harboring Illumina MiSeq sequencing adaptors were added in the second exponential PCR. Each individual sample was tagged with a barcoded (10 bp) fusion primer specific for the constant TCR genes. PCR amplicons were purified using the AmPure beads

(Beckman Coulter) and sequenced with MiSeq paired-end for 300 bp. After demultiplexing of the sequencing results, analysis of the TCR clonotypes was carried out using the MiMCR software. Calculation of the Shannon diversity index was performed to determine the richness of a population represented by its total number of species (for example CDR3 aa sequences). Shannon index was calculated as follows: $SA = -\sum_i (n_i/N) \lg (n_i/N)$, where i is an index that is chosen between 1 and the number of species s , n_i is the number of sequencing reads in species I , and N is the total number of reads.

Microarray analysis

T cells were isolated from total splenocytes of C57BL/6 (for co-culture with Ba/F3 cells) or C3H (for co-culture with 32D cells) donor mice, activated with anti-CD3/anti-CD28 conjugated beads (Dynabeads Mouse T-Activator CD3/CD28, Thermo Fisher Scientific), and then exposed to Ba/F3 cells (transfected with empty vector or JAK2^{V617F}) or 32D cells (transfected with JAK2 WT or JAK2^{V617F} vectors). T cells were isolated after 24 hours via FACS or MACS sorting. Total RNA was isolated using the RNeasy Mini kit (QIAGEN). Microarray analysis was performed on the resulting RNA. The complete gene expression data are available at ArrayExpress with the accession number E-MTAB-5028.

Affymetrix Clariom S Mouse arrays were normalized using Single-Channel Array Normalization and exon expression summarized to the gene expression using the R/Bioconductor package `pd.clariom.s.mouse` (Version 3.14.1). Differential pathway regulation was calculated using Gene Set Variation Analysis (GSVA), which maps gene expression to gene set activity per sample. Differences in pathway activity were then calculated using a moderated t-test via the R/Bioconductor package `limma`. For gene set definitions, we used the Molecular Signatures Database (MSigDB) collections v.5.2 that were

mapped to mouse ortholog Entrez IDs via the HGNC Comparison of Orthology Predictions (HCOP) (provided by the Walter and Eliza Hall Institute; <http://bioinf.wehi.edu.au/software/MSigDB/>). Gene sets with less than 10 or more than 500 members were discarded for statistical robustness and biological interpretation.

Analysis of metabolism-related genes: Pathways were selected from KEGG and Reactome gene sets containing the word “Metabolism”. Pathway activity and differential regulation were calculated via gene set variation analysis and a moderated t-test, respectively. Gene expression was scaled to have zero mean and unit standard deviation per row. Rows and columns were clustered according to their Euclidean distance using complete linkage.

Seahorse metabolism assays

Oxygen consumption rates (OCRs) and extracellular acidification rates (ECARs) were measured in XF medium (non-buffered RPMI 1640 containing 25 mM glucose, 2mM L-glutamine, and 1 mM sodium pyruvate) under basal conditions and in response to 200 μ M etomoxir (Tocris), 1 μ M oligomycin, 1.5 μ M fluoro-carbonyl cyanide phenylhydrazone (FCCP), and 100 nM rotenone + 1 μ M antimycin A, or 50 ng/mL phorbol 12-myristate 13-acetate (PMA) + 500 ng/mL ionomycin (all Sigma) using a 96-well XF or XFe Extracellular Flux Analyzer (EFA) (Seahorse Bioscience).

Immuno-positron emission tomography (PET)/computed tomography (CT) imaging and

analysis

ImmunoPET imaging after i.v. injection of 20 μg ^{64}Cu -NOTA-PD-L1 mAb (~ 8 MBq) was performed on mice with WT or JAK2^{V617F} transfected BM. Scans were acquired for 10-15 minutes with a minimum of 5 million counts. PET image reconstruction was performed with a routine 2D ordered subset expectation maximization (OSEM2D) algorithm provided by the scanner software for microPET Focus 120 (Concorde). CT scans were reconstructed with a T30 kernel and a resolution of 120 μm , using the manufacturer's software (Concorde). Fusion of the PET and CT images and the quantitative analysis of radiotracer uptake were performed with AMIDE software 1.0.5. The reported values represent the mean activity concentration expressed as percent injected activity per cubic centimeter of tissue (% IA/ cm^3).

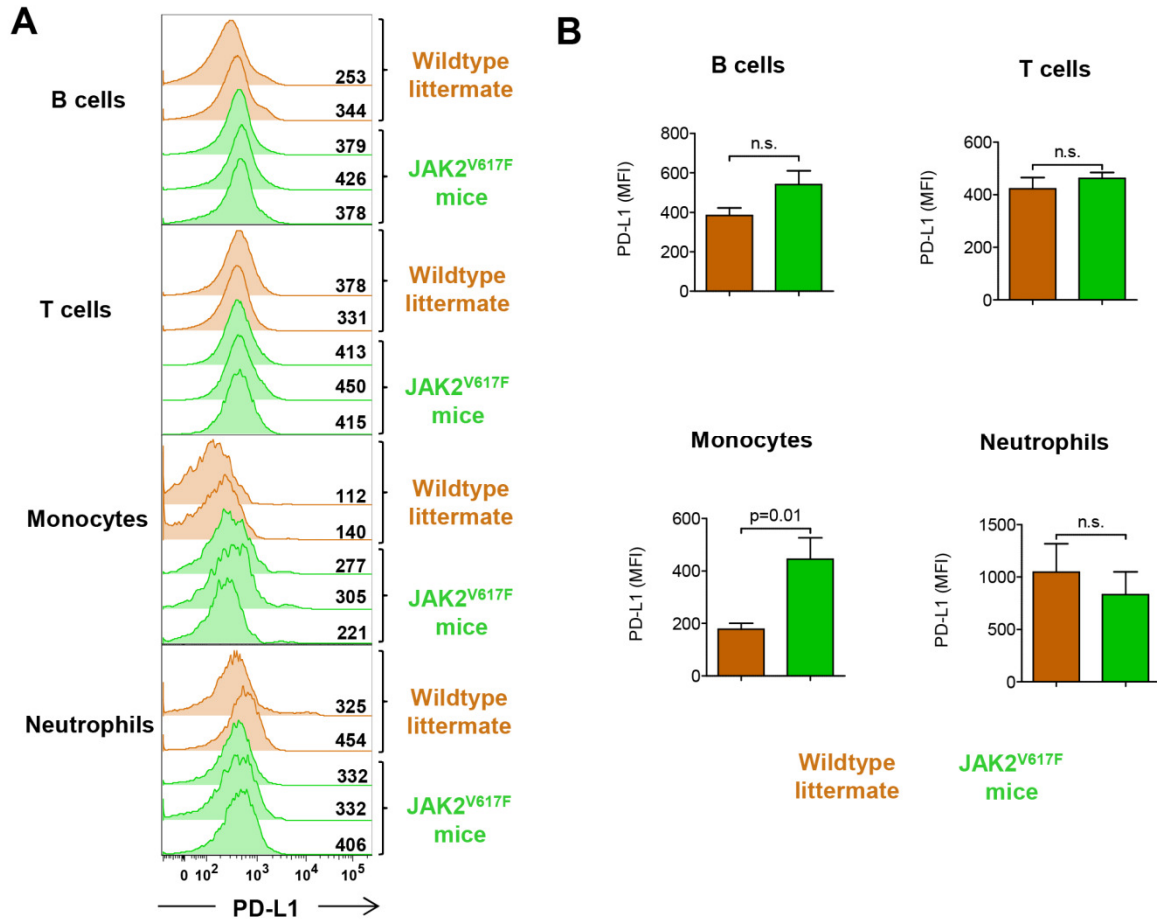
GVHD histopathology

Tissue sections of small intestine, colon, and liver were collected from recipient mice on day 7 after allo-HCT followed by hematoxylin/eosin (H/E) staining and GVHD grading on the basis of a histopathology scoring system ranging from 0 (no GVHD) to 4 (severe GVHD) for the small intestine, large intestine, and liver by an investigator blinded to the experimental groups.

Dilution of the antibodies for western blot

The following dilutions of the antibodies were used for western blots: anti-pSTAT1: 1:1000, anti-STAT1: 1:1000, anti-pSTAT3: 1:1000, STAT3: 1:1000, pSTAT5: 1:1000, STAT5: 1:1000. The following dilution of secondary antibodies were used: For phospho Abs: 1:2000 all anti rabbit, for total protein Abs: 1:10,000.

Suppl. Figure S1



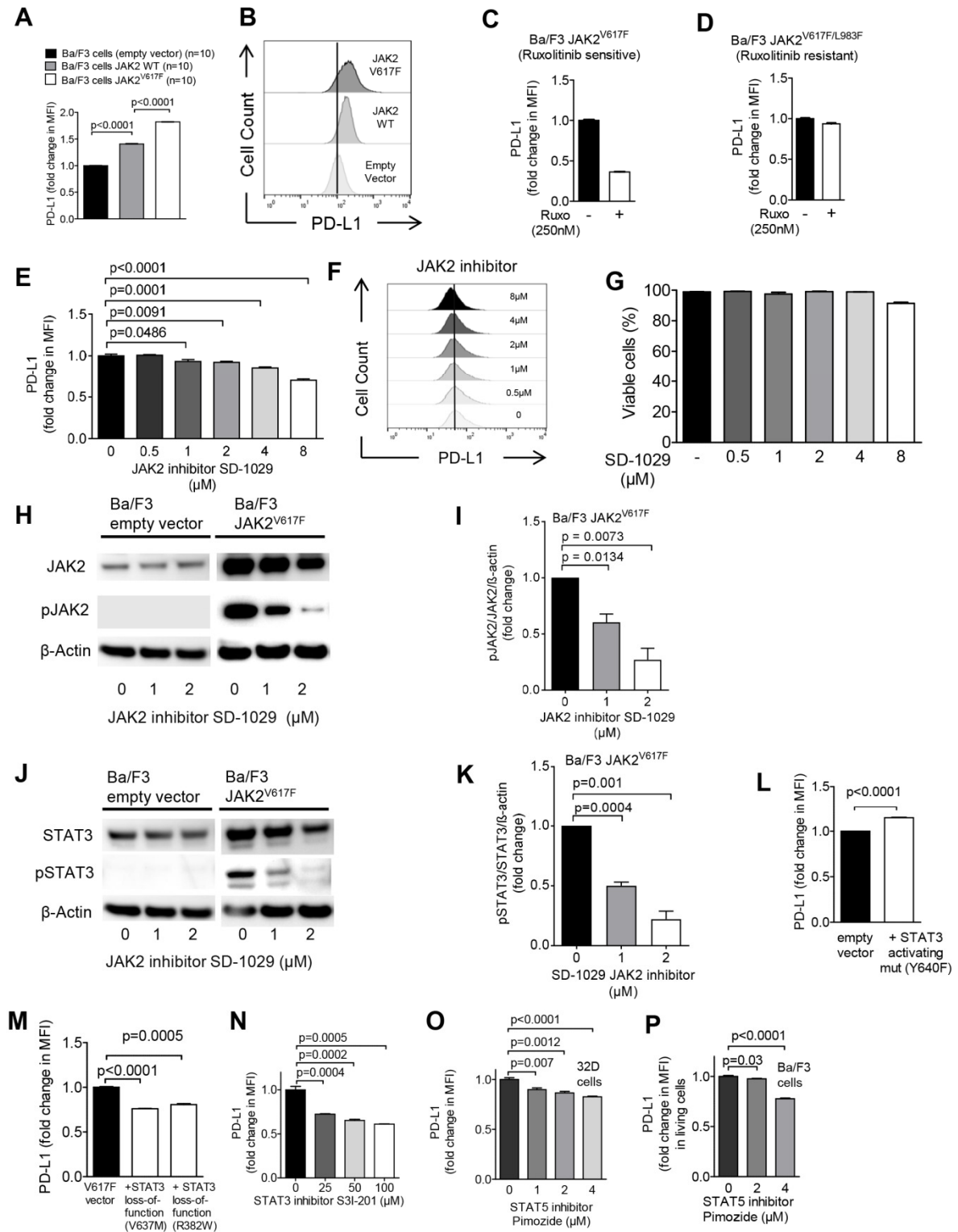
Suppl. Figure S1: PD-L1 expression is increased in JAK2^{V617F} primary mouse monocytes compared to wildtype mouse monocytes.

(A) Representative histograms show expression of PD-L1 on CD19⁺ B cells, CD90.2⁺ T cells, Ly6C⁺ monocytes, and Ly6G⁺ neutrophils harvested from the spleen of wildtype littermate (brown) and JAK2^{V617F} mice (green). Numbers show the PD-L1 expression (geometric mean) for each mouse. One of two independent experiments is shown.

(B) The bar diagrams show the PD-L1 expression (MFI) on the indicated cell types derived from the spleens harvested from wildtype littermate mice and JAK2^{V617F} mice. Data are

pooled from two independent experiments. A total of 5 littermate mice and 6 JAK2^{V617F} mice were analyzed.

Suppl. Figure S2



Suppl. Fig. S2: Oncogenic JAK2^{V617F} increases PD-L1 expression.

(A) PD-L1 expression as measured by flow cytometry on Ba/F3 cells transfected with an empty vector (control) or with a vector containing the gene for human JAK2 (either wild type or JAK2 carrying the activating mutation V617F). Data are pooled from 10 independent replicates.

(B) Representative histograms showing the expression of PD-L1 on Ba/F3 cells transfected as described in **(A)**.

(C, D) PD-L1 expression as measured by flow cytometry on Ba/F3 cells transfected with JAK2^{V617F} cells (ruxolitinib-sensitive) **(C)** or Ba/F3 JAK2^{V617F L983F} (ruxolitinib-resistant) **(D)** after exposure to ruxolitinib. Data are pooled from two independent experiments.

(E) The graph shows PD-L1 expression on Ba/F3 JAK2^{V617F} cells exposed to the specific JAK2 inhibitor SD-1029 at different concentrations. Data are pooled from three independent experiments.

(F) Histograms showing the expression of PD-L1 on Ba/F3 cells as described in **(E)**. The histograms are representative of three independent experiments.

(G) The bar diagram shows the percentages of viable Ba/F3 JAK2^{V617F} cells exposed to the specific JAK2 inhibitor SD-1029 at different concentrations.

(H) The Western blots display JAK2 total protein and phospho-JAK2 in Ba/F3 cells transfected with an empty vector or a JAK2^{V617F} vector and treated with the JAK2 inhibitor SD-1029 at the indicated concentrations. The blots are representative of three independent experiments.

(I) The bar diagram indicates the ratio of pJAK2/JAK2 normalized to the condition without JAK2 inhibitor (=1) of cells described in **(H)**. Pooled data from three independent experiments are displayed.

(J) The Western blots display STAT3 total protein and phospho-STAT3 in Ba/F3 cells transfected with an empty vector or a JAK2^{V617F} vector and treated with the JAK2 inhibitor SD-1029 at the indicated concentrations. The blots are representative of three independent experiments.

(K) The bar diagram indicates the ratio of pSTAT3/STAT3 normalized to the condition without JAK2 inhibitor (=1) of cells described in **(J)**. Pooled data from three independent experiments are displayed.

(L) The bar diagram displays the fold change of PD-L1 expression as measured by flow cytometry on Ba/F3 empty vector cells that were transfected with a vector containing a STAT3 activating mutation (Y640F) when indicated. Pooled data of two independent experiments are displayed.

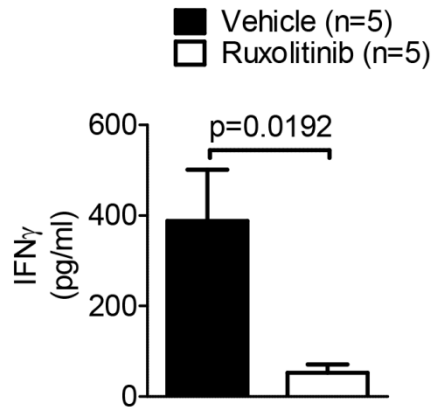
(M) The bar diagram displays the fold change of PD-L1 expression as measured by flow cytometry on Ba/F3 JAK2^{V617F} cells that were transfected with a vector containing two different STAT3 loss-of-function mutations (R382W or V637M) when indicated. Pooled data of two independent experiments are displayed.

(N) The bar diagram displays the fold change of PD-L1 expression as measured by flow cytometry on Ba/F3 JAK2^{V617F} cells after exposure to the STAT3 specific inhibitor S3I-201 at the indicated concentrations. Pooled data of two independent experiments are displayed.

(O) The bar diagram displays the fold change of PD-L1 expression as measured by flow cytometry on 32D JAK2^{V617F} cells after exposure to the STAT5 specific inhibitor pimoziide at the indicated concentrations. Pooled data of two independent experiments are displayed.

(P) The bar diagram displays the fold change of PD-L1 expression as measured by flow cytometry on Ba/F3 JAK2^{V617F} cells after exposure to the STAT5 specific inhibitor pimoziide at the indicated concentrations. Pooled data of two independent experiments are displayed.

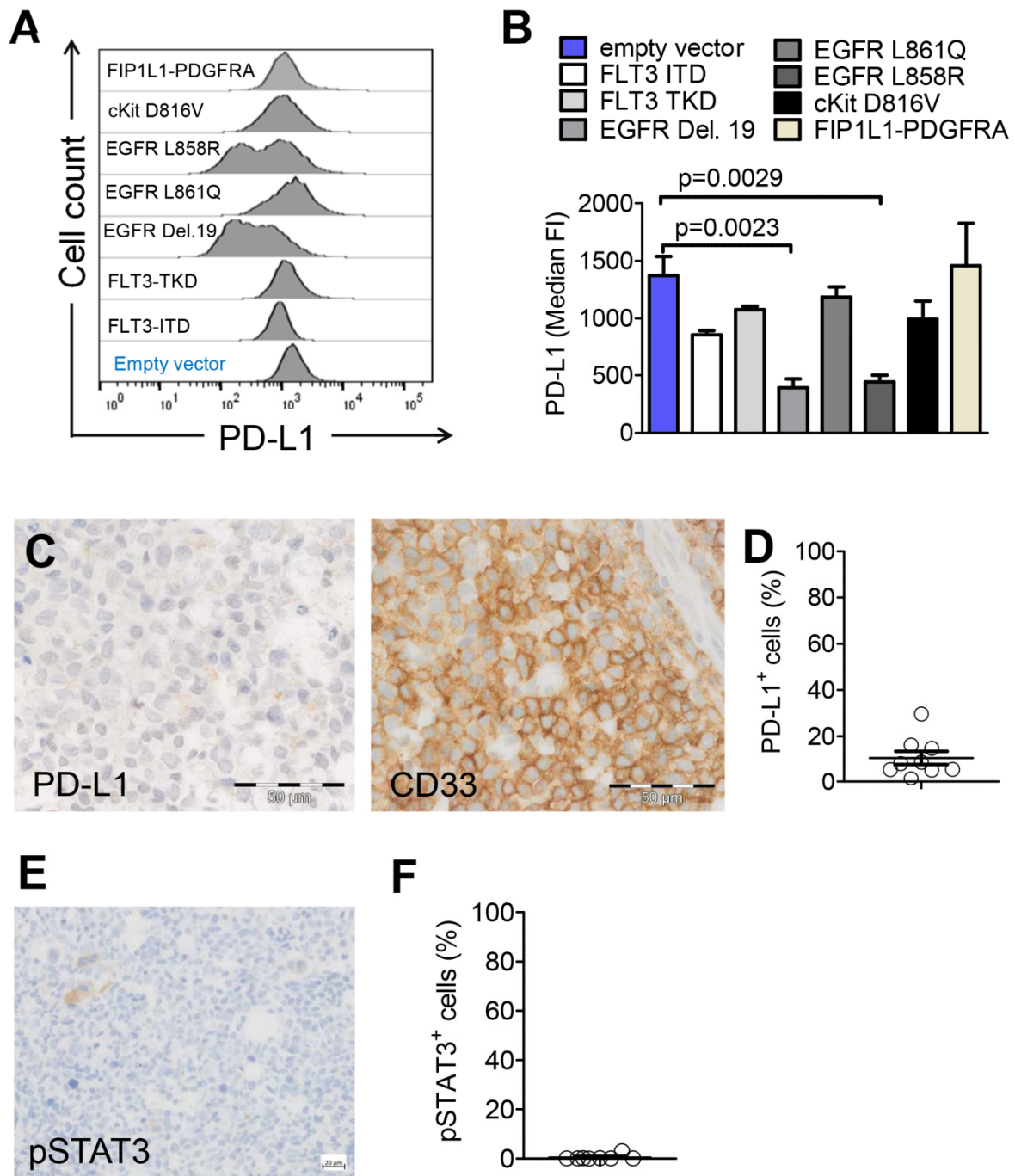
Suppl. Figure S3



Suppl. Fig. S3: Ruxolitinib treatment reduces serum IFN- γ in mice transplanted with JAK2^{V617F} transduced BM.

The bar diagram displays the IFN- γ serum concentration as measured by ELISA in the serum of mice that had received WT or JAK2^{V617F} transduced BM and treatment with vehicle or ruxolitinib (for 10 days) as indicated. Pooled data of two independent experiments are displayed.

Suppl. Figure S4



Suppl. Fig. S4: PD-L1 expression is not affected by different activating mutations.

(A) Representative histograms showing the expression of PD-L1 on 32D cells transfected with an empty vector (control) or with a vector containing the gene for different activating mutations including FLT3-ITD, FLT3-TKD, cKIT (d816v), EGFR (Del 19, L861Q, and L858R), or PDGFR (FIP1L1-PDGFR A). Data are pooled from 2 independent replicates.

(B) Bar diagrams showing the expression of PD-L1 on 32D cells transfected as described in **(A)**.

(C) Displayed is a representative bone marrow biopsy from an AML patient at diagnosis. The scale bar size represents 50 μm . Left image: PD-L1⁺ cells appear in brown. Right image: CD33⁺ cells appear in brown.

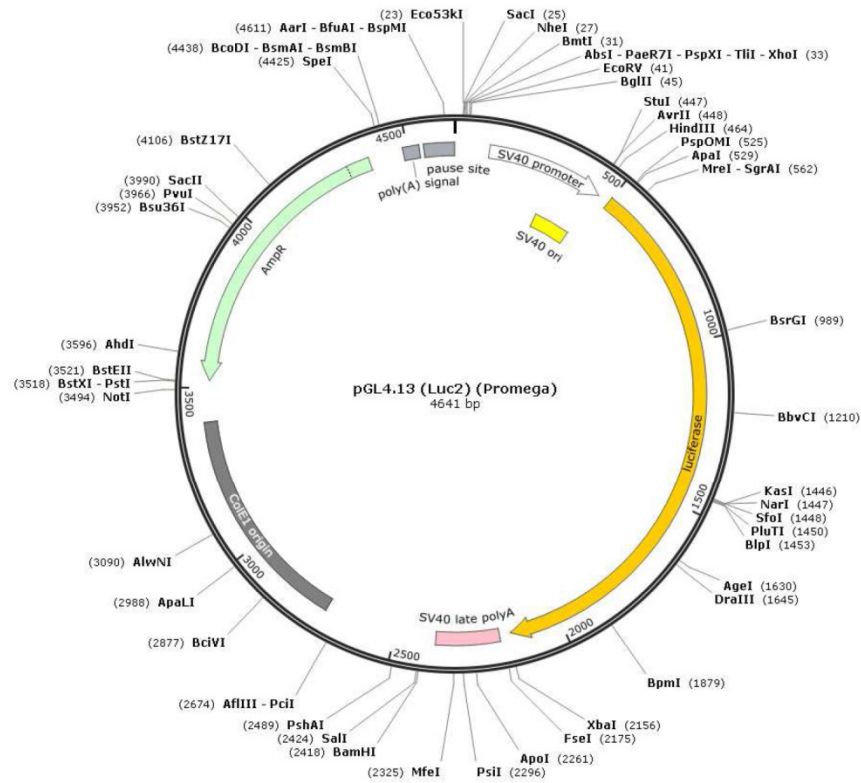
(D) The scatter plot diagram displays the number of PD-L1⁺ cells as a proportion of 100 cells (HPF, high power field) detected in bone marrow biopsies from 9 patients with AML at diagnosis.

(E, F) The image shows a representative AML sample stained against pSTAT3, the scale bar size represents 50 μm **(E)**, and the bar diagram **(F)** displays the number of pSTAT3⁺ cells as a proportion of 100 cells detected in bone marrow biopsies from 9 patients with AML at diagnosis.

Suppl. Figure S5

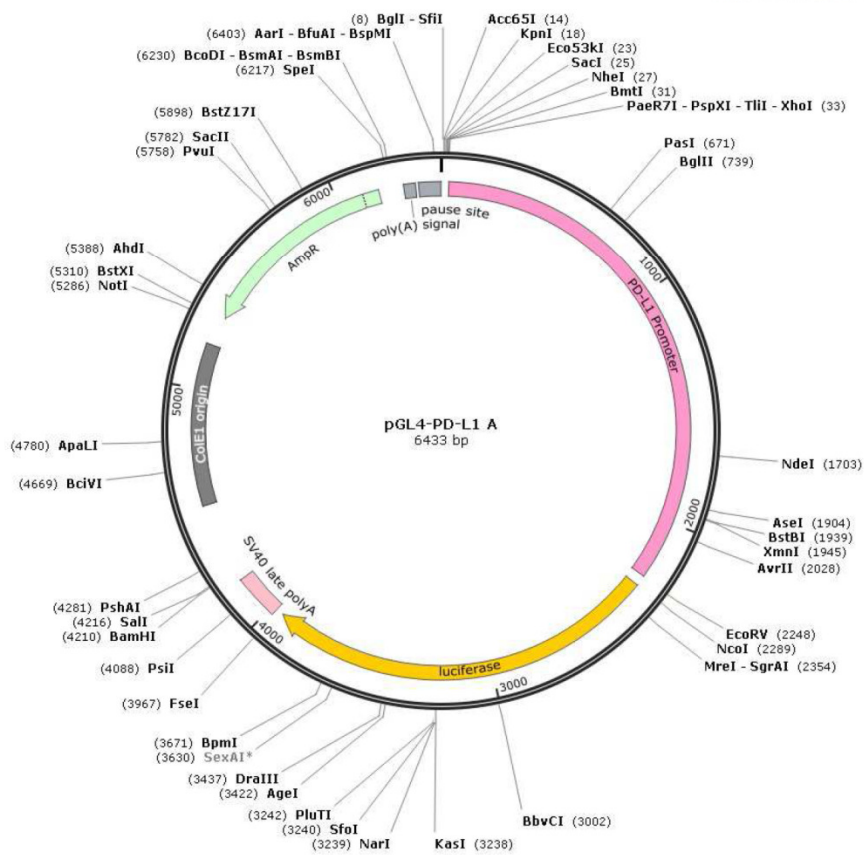
Created with SnapGene®

A



B

Created with SnapGene®

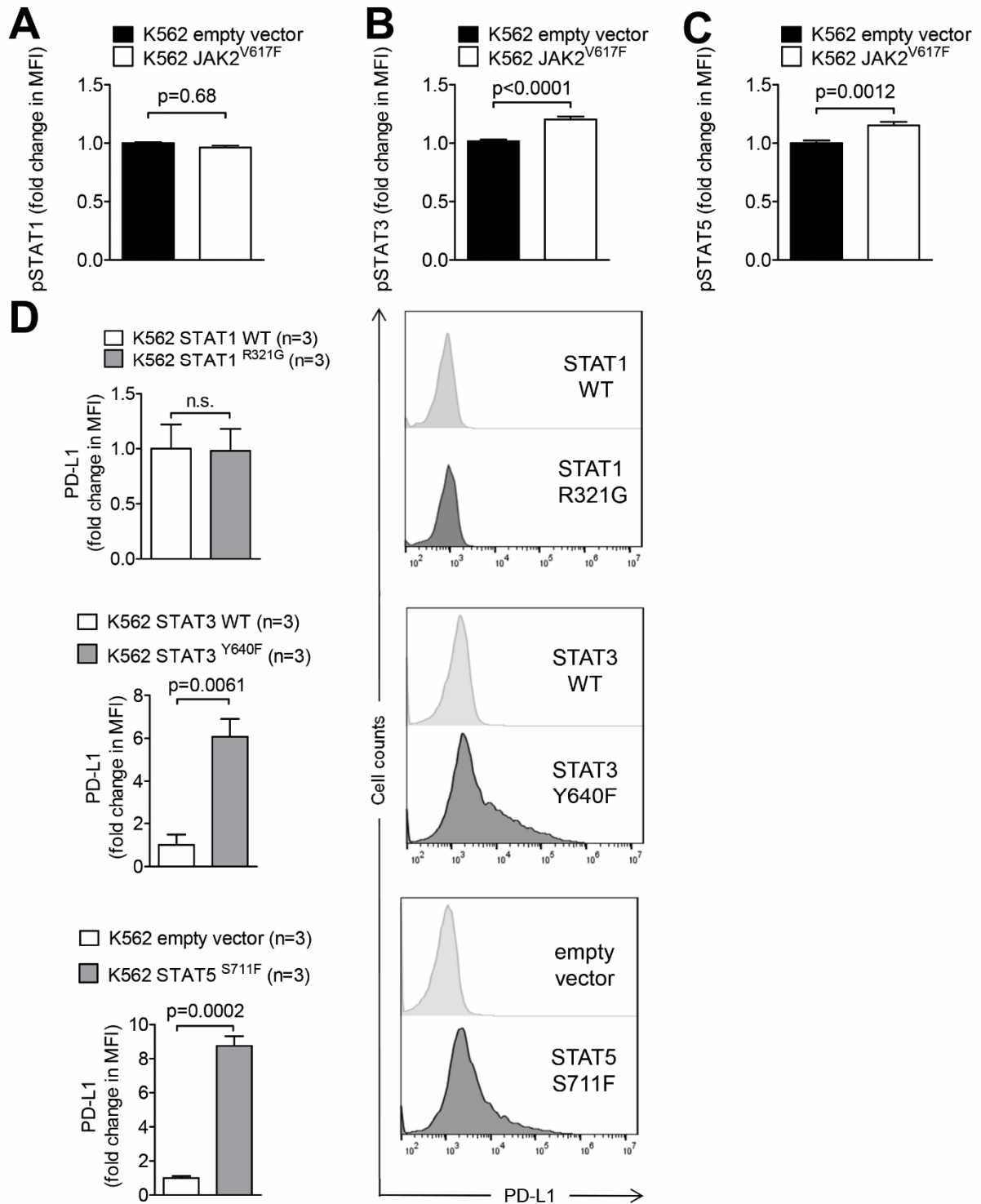


Suppl. Figure S5: The luciferase-reporter assay vector maps are displayed.

(A) The vector map shows the Luciferase Reporter Vector pGL4.13 [luc2/SV40] (Promega).

(B) The vector map shows the Luciferase Reporter Vector pGL4.14 after removing the SV40 promoter and cloning the PD-L1 promoter sequence into the blunt-ended promoterless vector.

Suppl. Figure S6

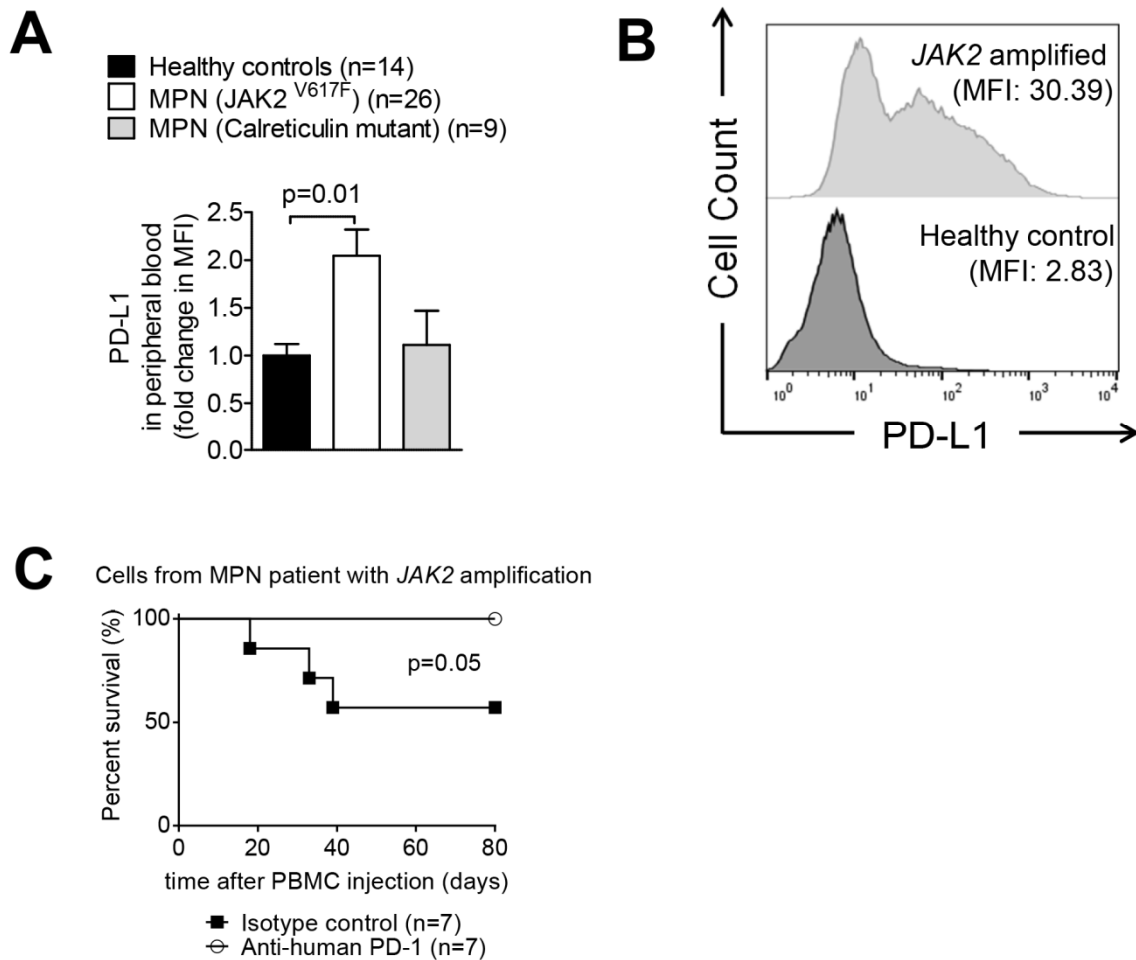


Suppl. Fig. S6: STAT3 and STAT5 activation increase PD-L1 expression.

(A-C) Amounts of pSTAT1 (A), pSTAT3 (B), and pSTAT5 (C) as measured by flow cytometry in K562 cells transfected with an empty vector (control) or with a vector containing JAK2^{V617F}. Data are pooled from 2 independent replicates.

(D) The bar diagrams display the fold change of PD-L1 expression as measured by flow cytometry on K562 cells that were transfected with a vector containing a STAT1 (R321G), STAT3 (Y640F), or STAT5 (S711F) activating mutation (GOF) as indicated. Pooled data of two independent experiments are displayed, with a representative histogram for each experimental setting.

Suppl. Figure S7



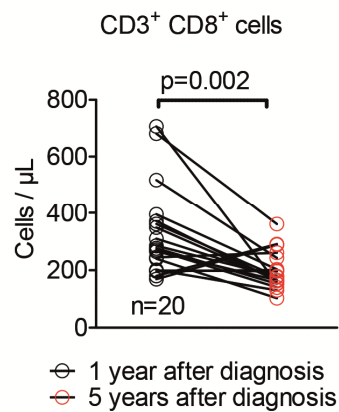
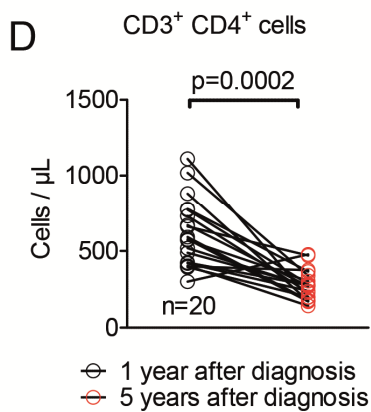
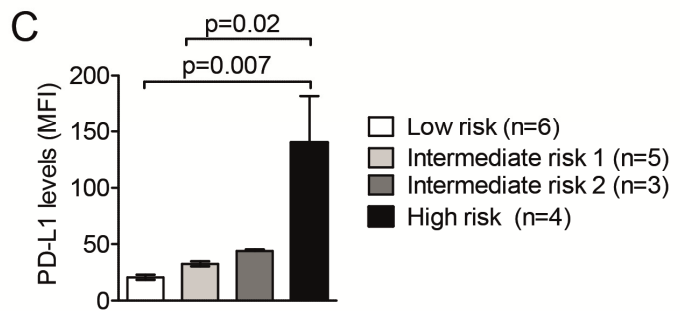
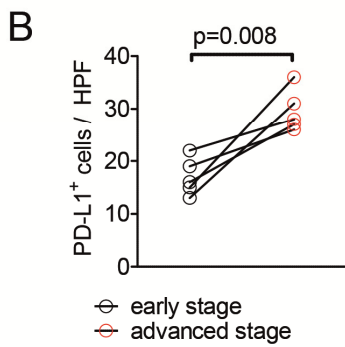
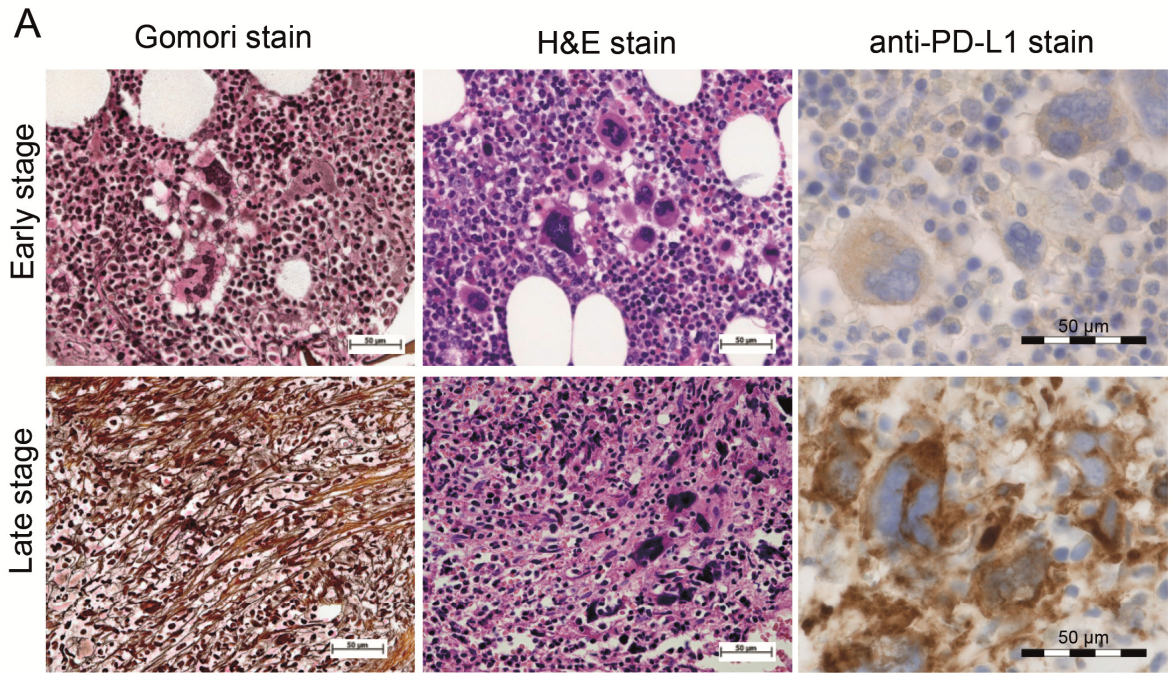
Suppl. Fig. S7: PD-L1 expression increases in human $JAK2^{V617F}$ mutant cells.

(A) The bar diagram displays the fold change of PD-L1 expression as measured by flow cytometry in peripheral blood cells and platelets from healthy volunteers, $JAK2^{V617F}$ MPN patients, or $CALR^{mut}$ MPN patients. The numbers of individuals in each group are shown in the figure.

(B) The histogram indicates the expression of PD-L1 on peripheral blood cells and platelets from a representative healthy volunteer and one patient with $JAK2$ amplification (amplification of chromosome 9).

(C) The survival of $RAG2^{-/-}Il2r^{-/-}$ mice after intravenous transfer of human PBMCs from a patient with a $JAK2$ amplification is shown. Mice were treated with 250 μ g of either isotype control Ab or anti-human PD-1 Ab on day 8 after PBMC injection. The numbers of mice for each group are shown (n=7). Data are pooled from two independent experiments.

Suppl. Figure S8



Suppl. Figure S8: PD-L1 expression depends on the MPN disease stage.

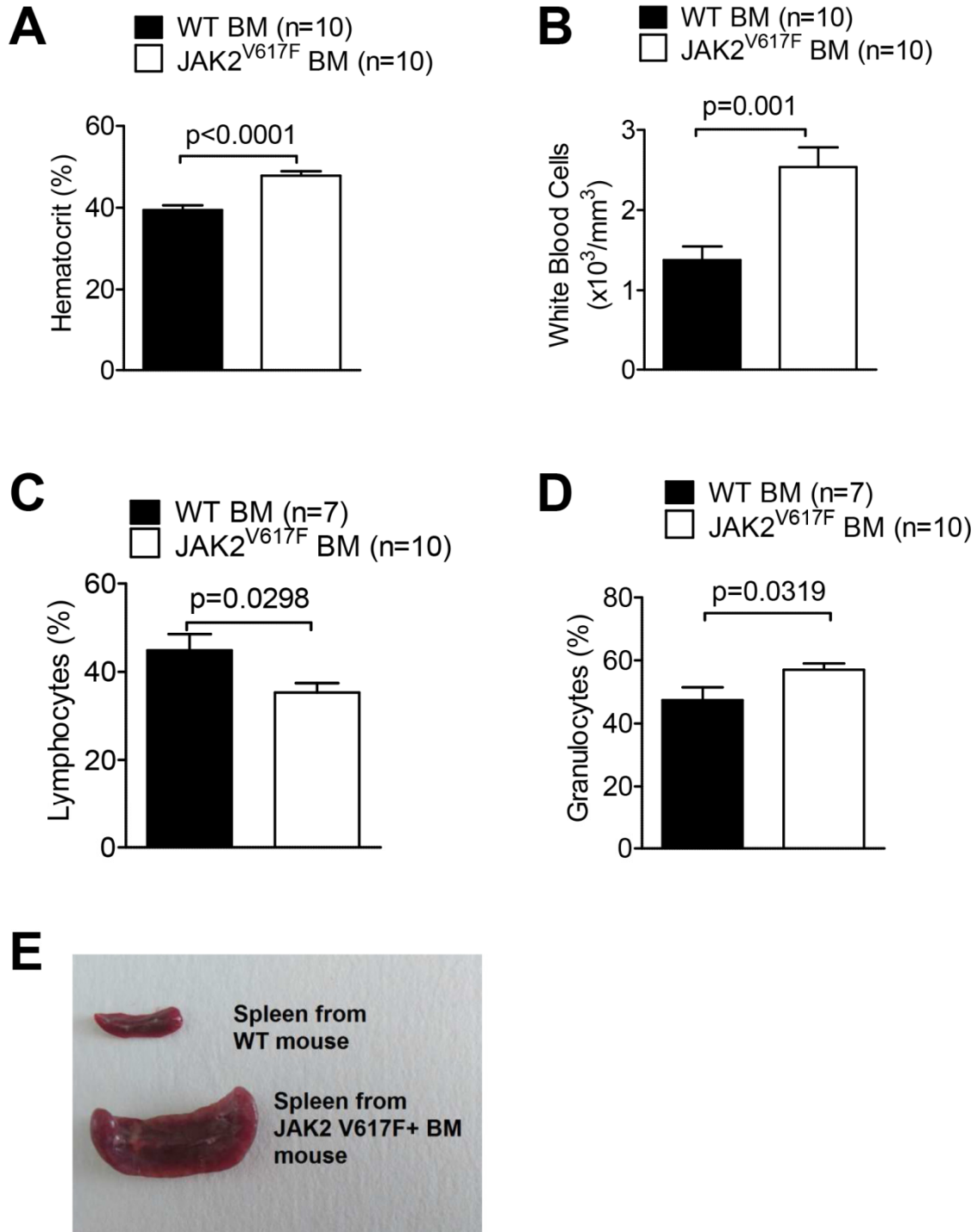
(A) Displayed is a representative bone marrow biopsy from a JAK2^{V617F} MPN patient at diagnosis (early stage, upper panel) and at advanced stage (lower panel). PD-L1⁺ cells appear in brown. Gomori stain, H&E stain. The scale bar size represents 50 μ m.

(B) The diagram shows the quantification of PD-L1 positive cells in bone marrow biopsies from JAK2^{V617F} MPN patients early (diagnosis) vs. late (5 years or more after diagnosis), per high power field. Each data point indicates the measurement of an individual patient at the indicated time point. *P* was determined using the Wilcoxon matched-pairs signed rank test.

(C) The diagram shows the quantification of MFI for PD-L1 on PBMCs in the PB from JAK2^{V617F} MPN patients stratified according to the DIPSS score. The number of patients is indicated for each group.

(D) The diagram shows the quantification of CD3⁺CD4⁺ and CD3⁺CD8⁺ cells (absolute numbers per μ l) in the peripheral blood from multiple JAK2^{V617F} MPN patients early (within 1 year of diagnosis) vs. late (5 years or more after diagnosis). Each data point indicates the measurement of an individual patient at the indicated time point. *P* was determined using the Wilcoxon matched-pairs signed rank test.

Suppl. Figure S9

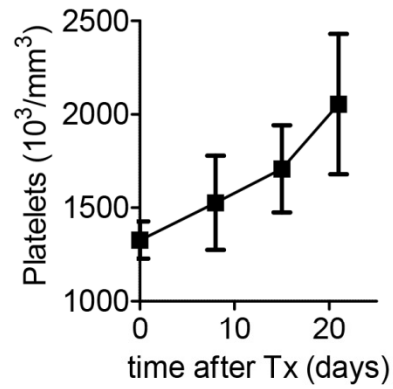


Suppl. Figure S9: Transfer of JAK2^{V617F} mutant BM results in MPN features.

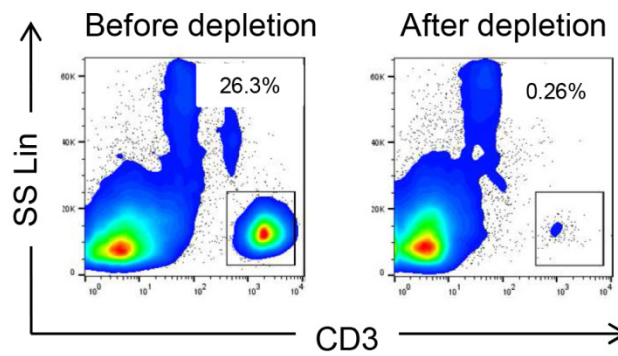
- (A) The bar diagram shows the hematocrit of BALB/c mice 11 days after transplantation of either JAK2^{V617F}-transfected or WT syngeneic BM.
- (B) The bar diagram shows the white blood cell count of BALB/c mice 11 days after transplantation of either JAK2^{V617F}-transfected or WT syngeneic BM.
- (C) The bar diagram shows the lymphocyte percentage of BALB/c mice 11 days after transplantation of either JAK2^{V617F}-transfected or WT syngeneic BM.
- (D) The bar diagram shows the granulocyte percentage of BALB/c mice 11 days after transplantation of either JAK2^{V617F}-transfected or WT syngeneic BM.
- (E) The image shows spleen sizes of a WT mouse and a mouse that had received JAK2^{V617F}-transfected BM.

Suppl. Figure S10

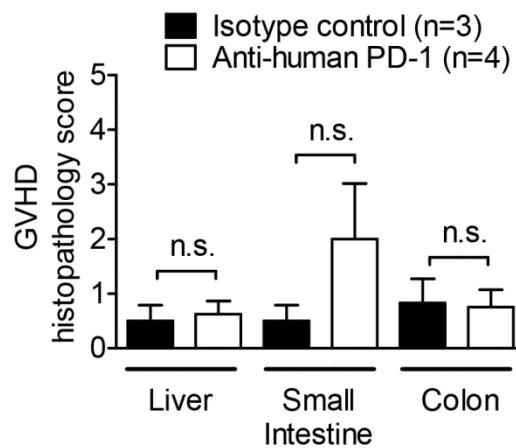
A



B



C



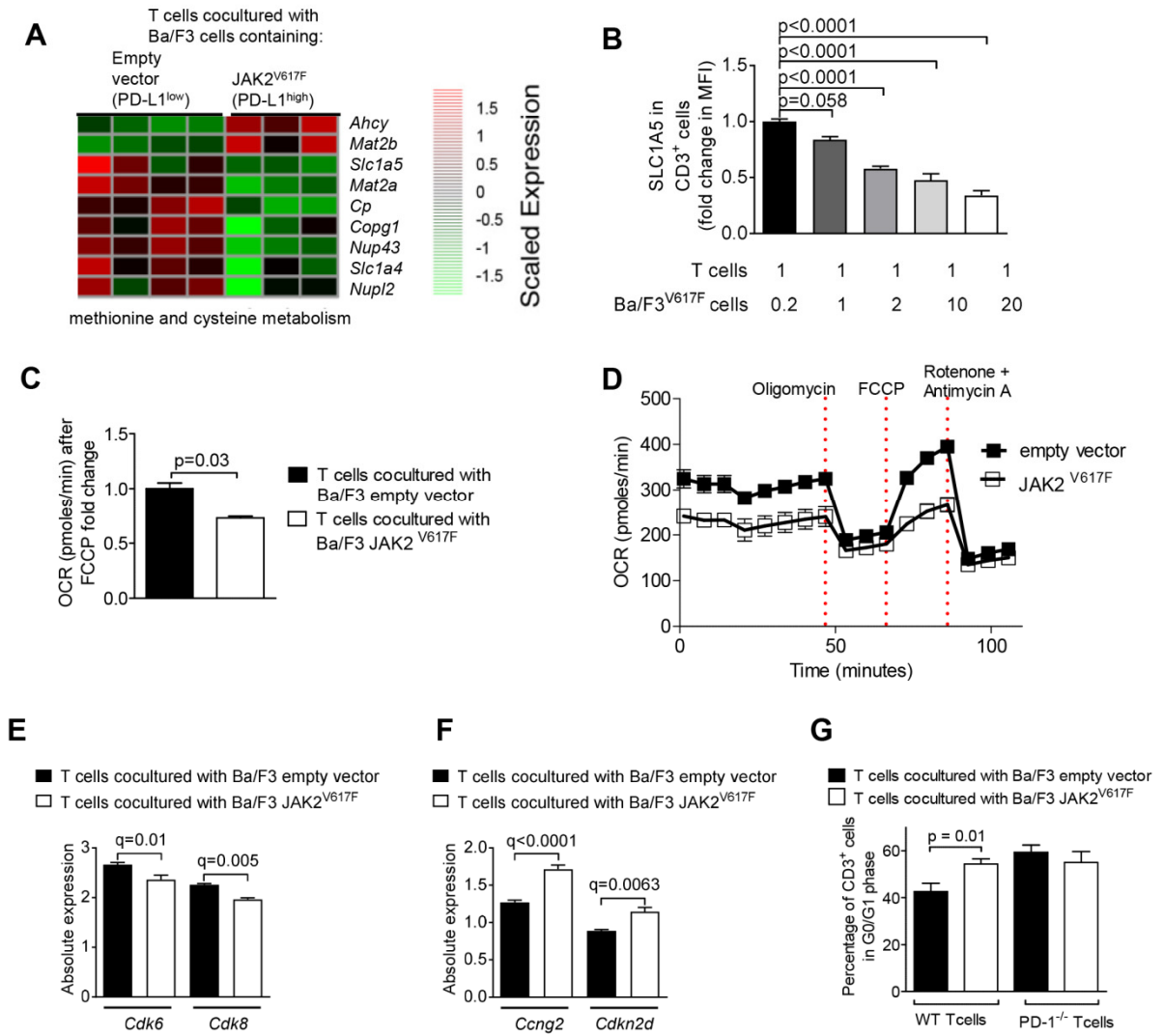
Suppl. Figure S10: Anti-PD-1 treatment does not increase GVHD scores.

(A) Platelet counts in the peripheral blood of *RAG2^{-/-}Il2r^{-/-}* mice at different time points after transfer of human PBMCs from an MPN patient are shown (MPN patient #1).

(B) The flow cytometry plot shows the percentages of CD3⁺ T cells before and after depletion of CD3 via MACS sorting.

(C) The GVHD histopathology scores for the liver, small intestine, and colon are shown for *RAG2^{-/-}Il2r^{-/-}* mice that had received human MPN cells, human T cells, and anti-PD-1 Ab or isotype IgG as indicated. The human PBMCs were from the MPN patient #1. The organs were isolated on day 20 after treatment.

Suppl. Figure S11



Suppl. Figure S11: JAK2^{V617F}-mutant Ba/F3 cells impact T cell metabolism and cell cycle.

(A) The heatmap represents the expression of genes involved in methionine and cysteine metabolism in T cells (C57BL/6) that were exposed to JAK2^{V617F} mutant or empty vector Ba/F3 cells (C3H) for 24 hours (n=4 empty vector and n=3 JAK2^{V617F} mutant Ba/F3 cells). Expression values are scaled to zero mean and unit variance across rows.

(B) Protein expression (MFI) of the amino acid transporter SLC1A5 in T cells that were exposed to JAK2^{V617F} mutant Ba/F3 cells at different ratios for 24 hours is shown. The cell numbers were as follows: T cells: always 100,000 cells / well; first bar: 20,000 Ba/F3 cells, T

cell:Ba/F3 cell ratio 1:0.2; second bar: 100,000 Ba/F3 cells, T cell:Ba/F3 cell ratio 1:1; third bar: 200,000 Ba/F3 cells, T cell:Ba/F3 cell ratio 1:2; fourth bar: 1,000,000 Ba/F3 cells, T cell:Ba/F3 cell ratio 1:10; fifth bar: 2,000,000 Ba/F3 cells, T cell:Ba/F3 cell ratio 1:20.

(C) OCR of T cells that were exposed to Ba/F3 cells with JAK2^{V617F} mutant or empty vector for 24 hours after FCCP exposure is shown. Data were combined from three experiments.

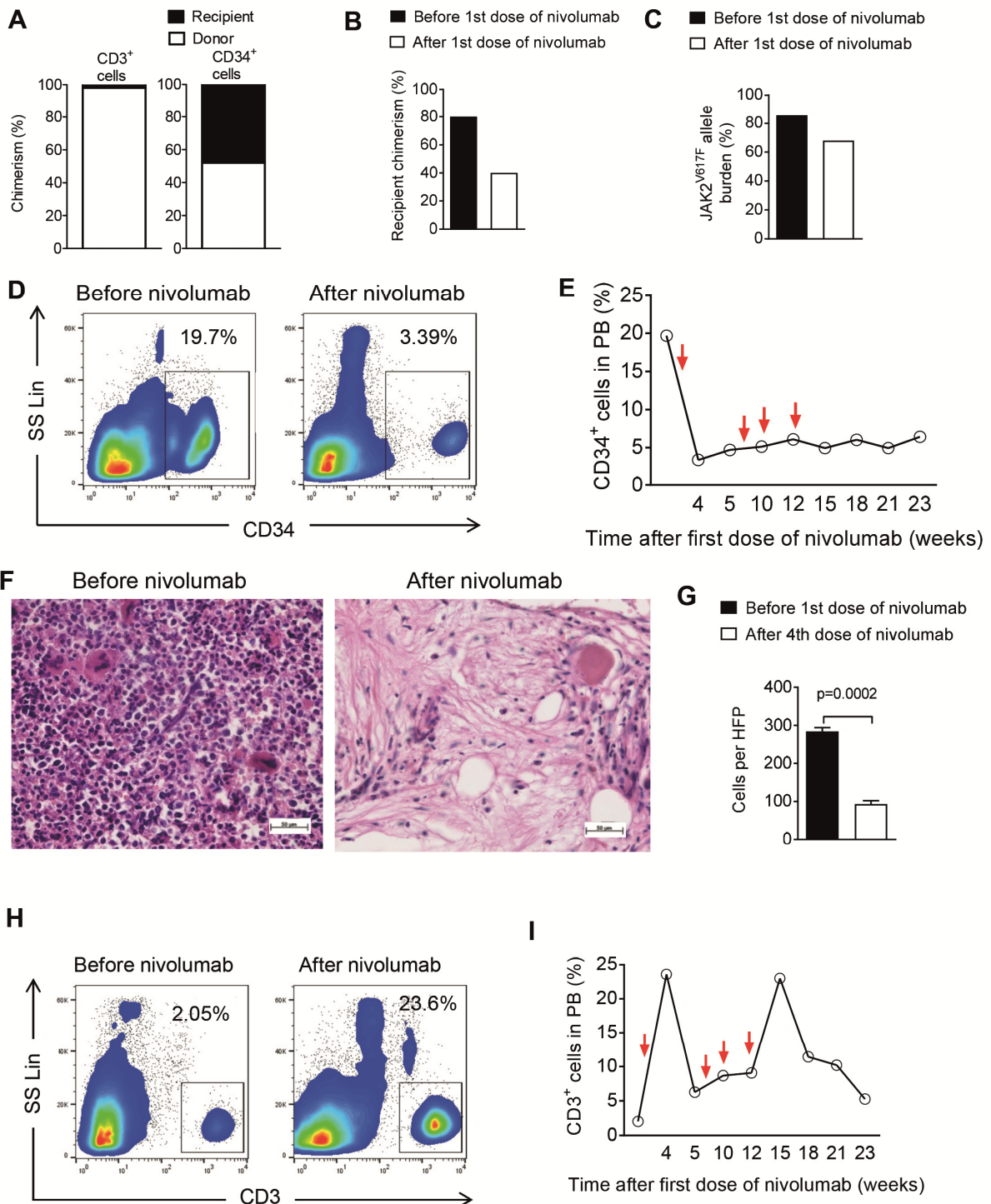
(D) Time course for OCR of T cells that were exposed to Ba/F3 cells with JAK2^{V617F} mutant or empty vector for 24 hours at baseline and after oligomycin, FCCP, and rotenone plus antimycin A exposure. The following compounds were used: oligomycin (ATP synthase inhibitor), FCCP (uncoupler), and rotenone/antimycin A (complex I and III inhibitors). Data were combined from three experiments.

(E) The bar diagram represents the expression of the *Cdk6* and *Cdk8* genes, which promote cell cycle progression, in T cells exposed to K562 cells with JAK2^{V617F} mutant or empty vector for 24 hours (n=4 empty vector and n=3 JAK2^{V617F} mutant Ba/F3 cells).

(F) The bar diagram represents the expression of the *Ccng2* and *Cdkn2d* genes, which inhibit cell cycle progression, in T cells exposed for 24 hours to Ba/F3 cells with JAK2^{V617F} mutant or empty vector (n=4 empty vector and n=3 JAK2^{V617F} mutant Ba/F3 cells).

(G) The bar diagram represents the percentage of CD3⁺ cells (WT or PD-1-deficient as indicated) that are in G0/G1 phase (non-cycling) when T cells were exposed for 24 hours to Ba/F3 cells with JAK2^{V617F} mutant or empty vector. The data are pooled from three independent experiments.

Suppl. Figure S12



Suppl. Figure S12: Anti-PD1 treatment decreases disease burden of an MPN patient.

(A) The bar diagram shows the percentage of donor chimerism in the CD3⁺ T cell and the CD34⁺ progenitor cell compartments in patient #1 before treatment with the anti-PD-1 antibody (details in table S2).

(B) The bar diagram shows the recipient chimerism in the peripheral blood before and after treatment with the anti-PD-1 antibody nivolumab.

(C) The bar diagram shows the JAK2^{V617F} allele burden in the peripheral blood before and after treatment with the anti-PD-1 antibody nivolumab. The JAK2^{V617F} allele burden was calculated as follows: $\text{JAK2}^{\text{V617F}} \text{ in } \% = \frac{\text{JAK2}^{\text{V617F}} \text{ copy numbers}}{(\text{JAK2}^{\text{V617F}} \text{ copy numbers} + \text{JAK2-WT copy numbers})} * 100$.

(D) The flow cytometry plot shows the percentages of CD34⁺ progenitor cells of patient #1 in the peripheral blood before and after the first treatment with the anti-PD1 antibody.

(E) The diagram shows the percentages of CD34⁺ progenitor cells of patient #1 in the peripheral blood at different time points relative to the treatment with the anti-PD1 antibody. Red arrows indicate treatment with the anti-PD1 antibody.

(F) A representative BM biopsy is shown before and after nivolumab treatment of patient #1. The scale bar size represents 50 μm .

(G) Cellularity of the BM biopsy per high power field is shown before and after nivolumab treatment of patient #1.

(H) The flow cytometry plot shows the percentages of CD3⁺ T cells in the peripheral blood before and after the first treatment with the anti-PD1 antibody (nivolumab 3 mg/kg body weight).

(I) The diagram shows the percentages of CD3⁺ T cells in the peripheral blood of patient #1 at different time points relative to the treatment with the anti-PD1 antibody. Red arrows indicate treatment with the anti-PD1 antibody.

Suppl. Table S1: JAK2^{V617F} MPN patients' characteristics

MPN patients shown in Fig. 3A (n=32)

Age (median/range)	61.52 (27-90)
	numbers (percentage)
Female	22 (69%)
Male	10 (31%)
PV	12 (37.5%)
ET	12 (37.5%)
PMF	8 (25%)
Splenomegaly	9 (28%)
	median (range)
WBC	12 (3.3 – 50.4)
Platelets	428 (43 - 1166)
Hb	13.2 (9.2 – 21.5)
No of previous treatments	1.5 (1 - 4) including phlebotomy , peginterferon, hydroxyurea, anagrelide, ruxolitinib, hydroxycarbamide, PBSCT
Duration of disease in months	69 (1 - 340)

MPN patients shown in Fig. 3 D and E (n=20)

Age (median/range)	59.9 (28-81)
	numbers (percentage)
Female	11 (55%)
Male	9 (45%)
PV	8 (40%)
ET	8 (40%)
PMF	4 (20%)

Abbreviations: MPN: myeloproliferative neoplasm, PV: polycythemia vera, PMF: primary myelofibrosis, ET: essential thrombocytosis

Suppl. Table S2: MPN patients for xenograft experiments

Patient #	Age	Gender	MPN subtype	JAK2 ^{V617F} +	conditioning	donor
1	72	male	PV	yes	FBM	sibling
2	74	female	PMF	yes	FBM	MUD
3	69	female	PV	yes	FBM	sibling

Abbreviations: MPN: myeloproliferative neoplasm, PV: polycythemia vera, PMF: primary myelofibrosis, FBM: fludarabine, BCNU: melphalan, MUD: matched unrelated donor.

All 3 patients had >60% donor chimerism in the T cell compartment at the time point when the PBMCs were isolated for xenograft experiments.

Suppl. Table S3: Antibodies

Abbreviations:

PB: Pacific blue

FITC: Fluorescein isothiocyanate

APC: Allophycocyanin

PE: Phycoerythrin

Cy: Cyanine

PerCP: Peridinin chlorophyll

Antibody	Clone	Catalogue number	Fluorochrome	Vendor
Anti-mouse CD3	17A2	17-0032	APC	eBioscience
Anti-mouse CD3	17A2	100214	PB	Biologend
Anti-mouse CD4	GK1.5	100434	PerCP/Cy5.5	Biologend
Anti-mouse CD8	53-6.7	560182	APC-H7	BD Pharmingen
Anti-mouse CD11b	M1/70	553311	PE	eBioscience
Anti-mouse CD19	6D5	115520	PE-Cy7	Biologend
Anti-mouse CD19	1D3	562291	PE-CF594	BD Bioscience
Anti-mouse CD34	MEC14.7	119308	PE	Biologend
Anti-mouse CD34	MEC14.7	152205	Alexa Fluor 647	Biologend
Anti-mouseCD41	MWReg30	133903	FITC	Biologend
Anti-mouse CD42d	1C2	148504	PE	Biologend
Anti-mouse CD44	IM7	103019	PB	Biologend
Anti-mouse CD45	30-F11	103126	PB	Biologend
Anti-mouse CD62L	MEL-14	104412	APC	Biologend
Anti-mouse CD62P	Psel.KO2.3	46-0626-82	PerCP eFluor 710	eBioscience
Anti-mouse CD90.2	53-2.1	140317	Brilliant Violet 605	Biologend
Anti-mouse Ly6G	1A8	127624	PE-Cy7	Biologend
Anti-mouse Ly6G	1A.8	127623	APC/Cy7	Biologend
Anti-mouse Ly6C	HK1.4	128014	Pacific Blue	Biologend
Anti-mouse PD-L1	10F.9G2	124311	APC	Biologend
ASCT2 Rabbit Ab	V501	5345S	-	Cell signalling
F(ab') ₂ fragment of goat anti-rabbit IgG		1683665	Alexa Fluor 647	Life Technologies
Anti-human CD3	HIT3a	300312	APC	Biologend
Anti-human CD3	SK7	344804	FITC	Biologend
Anti-human CD3	SK7	344824	PB	Biologend
Anti-human CD11b	M1/70	101224	PB	Biologend
Anti-human CD14	M5E2	561707	PE	BD Bioscience
Anti-human CD15	HI98	301908	APC	Biologend
Anti-human CD15	HI98	301904	FITC	Biologend
Anti-human CD19	HIB19	302207	PE	Biologend
Anti-human CD19	HIB19	302216	PE-Cy7	Biologend
Anti-human CD33	HIM3-4	303304	FITC	Biologend
Anti-human CD34	581	343506	PE	Biologend
Anti-human CD42b	HIP1	303903	FITC	Biologend

Anti-human CD45	HI30	304022	PB	Biologend
Anti-human CD45	HI30	304006	FITC	Biologend
Anti-human CD45	HI30	555483	PE	BD Pharmingen
Anti-human PD-L1/CD274	29E.2A3	329708	APC	Biologend
Anti-STAT1	pY701 clone 4a	612597	APC	BD Bioscience
Anti-STAT3	pY705 clone 4/P- STAT3	612569	PE	BD Bioscience
Anti-STAT5	pY694 clone 47/STAT5	612567	PE	BD Bioscience

Suppl. Table S4: Primer sequences (promoter assay)

Primers	Sequence
PD-L1_Promoter_SacI_fwd	5'-ACGTAGAGCTCTATCTAGCTCTTCAGCCCTGGCTCC-3'
PD-L1_Promoter_XhoI_rev	5'-ATGCAGCTCGAGGGACAGAAGCGCGGCTGGTGC-3'

Suppl. Table S5: Primer sequences (STAT1 mutagenesis)

Primers	Sequence
STAT1_KpnI_start_fwd (WT)	5'-GGTACCATGTCTCAGTGGTACGAACTTCA-3'
STAT1_BamHI_stop_rev (WT)	5'-GGATCCCTATACTGTGTTTCATCATACTG-3'
STAT1_961_A>G_fwd (R321G)	5'-TCGTTTGTGGTGGAAAGGACAGCCCTGCATGC-3'
STAT1_961_A>G_rev (R321G)	5'-GCATGCAGGGCTGTCCTTCCACCACAAACGA-3'